Radiation Physics and Chemistry 184 (2021) 109464

Contents lists available at ScienceDirect

Radiation Physics and Chemistry

journal homepage: www.elsevier.com/locate/radphyschem

Thymidine and stavudine molecules in reactions with low-energy electrons

M.V. Muftakhov, P.V. Shchukin *, R.V. Khatymov

Institute of Molecule and Crystal Physics - Subdivision of the Ufa Federal Research Centre of the Russian Academy of Sciences, Prospekt Oktyabrya 151, Ufa, 450075, Russia

ARTICLE INFO

Keywords:
Electron attachment
Nucleosides
Radiation damage
Thymidine
Stavudine
Radiosensitizers

ABSTRACT

The negative ion formation and fragmentation processes in thymidine and stavudine were studied by means of resonant electron capture mass spectrometry in the electron energy range 0–14 eV. Stavudine is a nucleoside analog of thymidine, that differs from the latter by the presence of double bond in the deoxyribose moiety. In the energy range below 5 eV transient negative ions have been found to arise via shape resonances resulting in electron attachment into the empty π*-orbitals. The main fragmentation channels for molecular ions are the H-atom loss and N-glycosidic bond cleavage between sugar and a nucleobase moieties. The dissociative electron attachment cross sections for the fragment negative ions were measured. The structures for some observed anions and neutral counterparts were suggested basing on the thermochemical approach for dissociative reactions energy balance under the support of quantum chemical calculations. The processes of ion formation in thymidine were found to be similar to those revealed previously for deoxyuridine nucleoside. In contrast, very strong dissociative channel was found for stavudine yielding $[M–R]^-$ ions (where R is a sugar moiety) in the energy range <3 eV. The efficient fragmentation found for stavudine in the low energy electron attachment reactions may have implications for the design of nucleoside radiosensitizers for cancer therapy.

1. Introduction

Over the two past decade, considerable interest has been attracted to the processes of resonance capture of low-energy electrons by biologically relevant molecules (Gorfinkiel and Ptasinska, 2017). It is assumed that these processes may play a crucial role in various biochemical reactions occurring in living organisms. The abundance of low-energy electrons in living media may be originated both by external impact, *e.g.* ionizing radiation which is shown to produce 10^4 electrons per 1 MeV (Cobut et al., 1998), and by internal biochemical processes, such as those occurring in the mitochondrial respiratory chain (Jian-Xing, 2015). One of the prominent features of electron attachment processes is their capability to initiate the destruction of molecules at electron energies well below ionization thresholds, even at zero energy. That the secondary low-energy electron attachment reactions play an important role in DNA radiation damage via single- and double-strand breaks it became evident after the eminent work of Sanche et al. (Boudaiffa et al., 2000). This work gave impetus for extensive gas-phase studies on resonant electron capture by building blocks of DNA such as nucleobases (Aflatooni et al., 1998; Denifl et al., 2004a, 2004b; Gohlke et al., 2003; Ptasińska et al., 2005a; Huber et al., 2006; Hanel et al., 2003)–(Aflatooni et al., 1998; Denifl et al., 2004a, 2004b; Gohlke et al., 2003; Ptasińska et al., 2005a; Huber et al., 2006; Hanel et al., 2003), sugars (Ptasińska et al., 2004; Bald et al., 2006; Sulzer et al., 2006) and phosphates (König et al., 2006) for better comprehension of damage mechanisms.

Motivated by the same intent, the resonant electron attachment studies were expanded to cover other biologically relevant molecules, such as amino acids (Gohlke et al., 2002; Ptasińska et al., 2005b; Vasil'ev et al., 2006) and peptides (Muftakhov and Shchukin, 2011; Kopyra et al., 2013). To date, the main mechanisms of electron capture and molecular negative ions' characteristic decay pathways have been established. Currently, in addition to fundamental challenges, research in this area is aimed at solving a number of applied problems. Among them, the well known fact that some of these molecules or their derivatives possess medicinal properties is awaiting for its comprehensive explanation, and the studies by means of low-energy electron-molecule interactions may shed light to molecular mechanisms underlying their therapeutic effect. Nucleosides, the molecules assembled from nucleobase and sugar groups, serve as building blocks of DNA molecule. The nucleoside derivatives have been widely used as antiretroviral drugs for treatment HIV (Kukhanova, 2012) and anti-cancer agents both for chemotherapy and radiosensitizing (Seley-Radtke and Yates, 2018; Lee

* Corresponding author.
E-mail address: pavel@anrb.ru (P.V. Shchukin).

https://doi.org/10.1016/j.radphyschem.2021.109464
Received 29 July 2020; Received in revised form 9 March 2021; Accepted 25 March 2021
Available online 31 March 2021
0969-806X/

et al., 2013). Currently, research is being conducted on their use for the treatment of coronavirus infections (Pruijssers and Denison, 2019), including COVID-19 (Babadaei et al., 2020). Thus, in view of widespread of problems of vital significance they cover, nucleosides certainly deserve special attention and comprehensive investigation. But, unlike their both building blocks as separate, molecules of nucleobases and sugars, electron attachment to nucleoside molecules have not been examined in depth yet. The major hurdle for gas-phase experiments with biomolecules is posed by their thermolability, the relatively low decomposition temperature that inhibits their effective sublimation intact when heating.

In our experiments, we use a technique in which the test sample is vaporized directly in the ionization chamber. This allows us to obtain the required vapor densities at lower temperatures, which prevents its thermal decomposition. Here we report a comprehensive study of low-energy electron molecule reactions with thymidine, one of the four basic nucleoside in DNA. DNA contains the thymidine instead of uridine, which is presented in RNA and was studied in detail in our earlier work together with deoxyuridine (Muftakhov and Shchukin, 2019). The processes of resonant electron attachment to thymidine were studied earlier in works (Ptasińska et al., 2006; Abdoul-Carime et al., 2004a) and intense fragmentation channels were found associated with H-atom loss and the N-glycosidic bond breakage. Besides, we also investigate stavudine, the nucleoside analog of thymidine. It differs in structure from thymidine by the replacement of the 3'-hydroxyl group with a hydrogen atom and by a doubled bond in the 2',3'-positions on the deoxyribose ring.

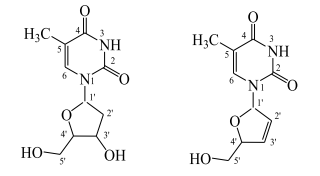

Stavudine is antiretroviral drug used for treating and preventing HIV infection. As for principle of its action, due to close structural similarity with thymidine, stavudine tends to be mistakenly recognized by a virus and incorporated instead of thymidine into the viral DNA. This results in termination of chain replication because of the lack of required OH-group in 3'-site, responsible for mutual linking the adjacent nucleotides (Hurst and Noble, 1999). The present work is aimed mainly at assessment of general stability of thymidine and stavudine against exposure to low-energy electrons, what may represent key importance for radiation chemistry, medicine, pharmaceuticals and other fields.

2. Experimental

The experiment was performed using MI-1201B commercial magnetic mass spectrometer (Ukraine, Sumy) modified for the investigation of negative ions formation under the controlled resonant electron capture conditions. The apparatus has been described in detail elsewhere (Mazunov et al., 2006). Briefly, an electron beam emitted from the thoriated tungsten cathode passed through ionization chamber, where it interacts with the vapor of the substance under investigation. The negative ions formed via resonance electron capture reactions are extracted from the ionization chamber by a weak electrostatic field, accelerated, mass selected with the magnetic-sector analyzer and detected by a secondary electron multiplier. A signal for the mass-selected negative ions are recorded as a function of electron energy in the 0-14 eV range. The samples of nucleosides were loaded directly into the bottom of ionization chamber and evaporated by heating it. This technique makes it possible to evaporate the sample at a lower temperature, preventing thermal degradation of compound. The optimal evaporation temperatures were 138°C for thymidine and 112°C for stavudine. The electron energy scale was calibrated whereby positions of the maxima in the yield curves of negative ions SF_6^-/SF_6 (~0 eV) and $[M–H]^-/CH_3COOH$ (~1.55 eV (Muftakhov et al., 1999)). The energy spread of the electron beam was estimated to be 0.4 eV at an electron current of about 0.5 μA. The negative ions appearance energies (AE_{exp}) were measured as energy shift from the of SF_6^-/SF_6 peak's onset, taken as zero for AE_{exp} energy scale. The dissociative electron attachment cross sections were measured with a mass spectrometric procedure described elsewhere (Khatymov et al., 2003). Briefly, the procedure is based on comparing the cross-sections of the compound under study with the known cross-section of the reference sample, which is also injected during the experiment. In order to estimate the difference in the vapor densities of both compounds, the mass spectra of electron ionization are recorded. In contrast to negative ions, the formation cross sections of the positive ions for different compounds differ little from each other being of the order of 10^{-15} cm^2. Therefore, a comparison of the integral intensity of the recorded positive ions mass spectra of the studied and reference compounds makes it possible to estimate the ratio of their inlet abundance. Knowing this ratio, other things being equal, it is possible to estimate the unknown formation cross-section for negative ions. The samples purchased from Sigma/Aldrich Chemical Co. with a stated purity of 99% or greater (Thymidine, $C_{10}H_{14}N_2O_5$, molecular weight MW = 242.23 g/mol) and 98% (Stavudine, $C_{10}H_{12}N_2O_4$, MW = 224.21 g/mol) were used without further purification.

3. Computational details

When analyzing possible pathways of dissociative electron capture reactions, we refer to theoretical calculations of the fragment negative ions appearance energies of (AE_{calc}), comparing them with experimentally measured values (AE_{exp}). The dissociative electron attachment reactions $e^- + AB \rightarrow AB^{\#-} \rightarrow A^- + B$ occur above the energy threshold generally described by the energy balance equation(Khvostenko, 1981):

$$AE_{calc}(A^-) = D(A–B) – EA(A) + E^* = \Delta H_f^0(A^-) + \Delta H_f^0(B) – \Delta H_f^0(AB) + E^*,$$

where D (A–B) is the homolytic A–B bond dissociation energy, EA(A) is the electron affinity of the A counterpart, ΔH_f^0 is the standard enthalpy of formation, E* is an excess energy of the process released as the excitation energy of fragments and their kinetic energy. Because it is hardly possible to determine theoretically the value of excess energy E*, this term was neglected, thereby the obtained AE_{calc} values representing the lower limits of thermodynamic thresholds for each suggested dissociative reaction. The enthalpies ΔH_f^0 (listed in Table S1, supplementary material) were computed using X1 method (available on the web (http://www.xdft.org/dft/X)) which combines the density functional theory with a neural network correction for an accurate prediction of heats of formation. (Wu and Xu, 2007) The optimized geometry of the species, the zero-point energy and thermal corrections required to estimate the enthalpies were calculated at the B3LYP/6-311+G (d,p) level of theory and the total energy was taken from B3LYP/6-311+G (3df,2p) single point energy calculations. To interpret the resonant states associated with occupation of normally empty molecular orbitals, the virtual orbital energies (VOEs) of the neutral molecules were evaluated using the B3LYP hybrid functional with the standard 6-31G(d) basis set. For predicting vertical attachment energies (VAEs) the VOEs were scaled using the linear equation VAE = (VOE + 1.14)/1.24. (Scheer and Burrow, 2006) All quantum chemical calculations were performed using the Firefly software package, (Granovsky,) partially based on the GAMESS (US) software code. (Schmidt et al., 1993)

4. Results and discussion

4.1. Thymidine

The electron attachment to thymidine molecules occurs in a wide range of electron energy 0–14 eV giving rise to deep multichannel fragmentation. As many as thirteen fragment negative ion peaks were detected in mass spectrum. The effective yield curves of these ions recorded as functions of electron energy are plotted in Fig. 1. Alike for deoxyuridine, no long-lived molecular anions are observed, apparently owing to insufficiency of electron affinity (EA) of thymidine molecule, which is known to amount 0.4 eV (Stokes et al., 2007). Besides, the yield of parent anions, being expected at thermal electron energy (close to zero), might be suppressed by the competing factors, such as an efficient fragmentation, what is evidenced by the presence of abundant fragment ion peaks at zero energy (Fig. 1). It is worth to oppose to the uridine possessing greater EA = 0.7 eV (Muftakhov and Shchukin, 2013) which in previous studies exhibited long-lived parent anions peaked at thermal electron energy despite the interference of efficient fragmentation (Muftakhov and Shchukin, 2013). In full agreement with earlier reports (Ptasińska et al., 2006; Abdoul-Carime et al., 2004a), the dominating peaks in the mass spectrum of thymidine at m/z = 241 and 125 pertain to $[M–H]^-$ and $[M–R]^-$ ions, respectively (where M stands for a target parent molecule and R stands for $C_5H_9O_3$ neutral counterpart representing dehydrogenated deoxyribose), and to newly found OCN^- ions (m/z = 42). Remaining fragment ions are far less abundant, yielding predominantly at energies above 5 eV.

The negative ion mass spectrum of thymidine bears close similarities to the spectrum of previously studied deoxyuridine (Muftakhov and Shchukin, 2019), a nucleoside with the only difference in the hydrogen atom instead of 5-methyl group. The similarity lies both in the resonance features and the fragmentation pattern. It is not surprising that the total dissociative electron attachment cross-section for thymidine at energies >5 eV is almost identical to that of deoxyuridine, being no more than 1.1 times smaller. For direct comparison, partial dissociative electron attachment cross section measured for the $[M–R]^-$ ions at peak maxima 6.4 eV is 9×10^{-19} cm^2 (Fig. 1), while anions emerging from deoxyuridine by analogous expelling deoxyribose moiety form similarly shaped peak at 6.45 eV (continued by a shoulder at 7.5 eV) (Muftakhov and Shchukin, 2019) with the comparable cross section of ca. 11×10^{-19} cm^2 (unpublished data). Therefore, it seems prudent to pursue the interpretation of the data on dissociative electron attachment for thymidine based on a comparison of the mass spectra of these two nucleosides, as well as on the results of similar studies for its separate moieties, molecules of thymine (Denifl et al., 2004b) and deoxyribose (Shchukin et al., 2013). Structures for identified fragment ions from thymidine are shown in Fig. 1.

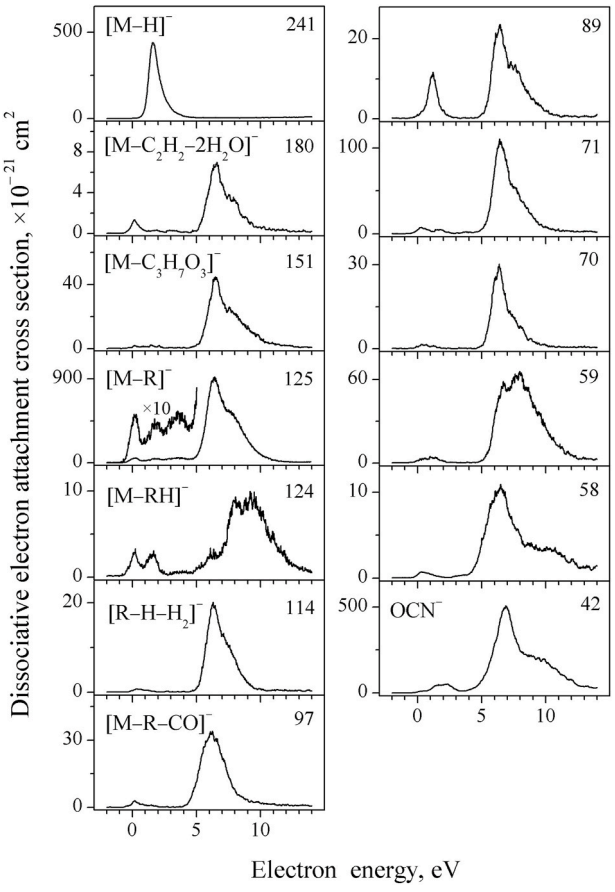

Fig. 1. Formation cross sections of negative ions from thymidine as functions of electron energy. The ions mass numbers (m/z) are indicated. The R stands for $C_5H_9O_3$ neutral counterpart representing dehydrogenated deoxyribose.

As can be seen, the resonant electron capture by thymidine gives rise to manifold dissociative channels some of which may result in ions of isobaric elemental composition. In addition to the abovementioned dehydrogenation and N-glycosidic bond rupture yielding $[M–H]^-$ and $[M–R]^-$ ions, the nucleobase and sugar moieties in thymidine undergo fragmentation as well. Thus, the decay of nucleobase is evidenced by the yield of OCN^- ions (m/z 42), $[M–R–CO]^{\bullet-}$ (m/z 97), while the ions $[M–C_2H_2–2H_2O]^{\bullet-}$ (m/z 180), $[M–C_3H_7O_3]^-$ (m/z 151) testify to the destruction of sugar ring. The negative ions with m/z 114, 89, 70, 59, and 58 should apparently be associated with fragmentation of sugar, because the similar species were detected in the mass spectrum of ribose (Shchukin et al., 2013) while they were not observed for thymine (Denifl et al., 2004b). Unambiguous identification of the elemental composition and structure of these negative ions is hardly possible since several alternative candidates can be hypothesised.

The ions with m/z 124 are readily attributed to $[M–RH]^-$ under the assumption of N-glycosidic bond rupture accompanied with the pyrimidinic C_6-site hydrogen atom shift toward expelled sugar counterpart (Fig. 2a). Despite a relatively low threshold energy assessed at 0.33 eV, this reaction produces weak ion yield, apparently due to the suppression by competing routs, both other dissociative channels and electron autodetachment. Indeed, by mere considerations, bond rupture accompanied by H-shift requires longer time to elapse compared to simple rupture of N-glycosidic bond giving rise to an orders of magnitude more abundant $[M–R]^-$ ions all over the equatable resonance peaks (Fig. 1).

Of the greatest interest is the study of dissociative electron attachment to thymidine in the low energy range (<3 eV), as it is important for biochemical issues. As seen from Fig. 1, there are two predominant dissociation channels at these energies, that lead to the abundant formation of $[M–H]^-$ and $[M–R]^-$ negative ions. The $[M–H]^-$ ions can be produced through hydrogen atom loss from both the thymine and sugar moieties of the nucleoside. However, a comparison of the dissociative electron attachment cross sections for $[M–H]^-$ ions from thymidine $4.4\text{x}10^{-19}$ cm^2 and thymine $1.1\text{x}10^{-18}$ cm^2 (unpublished data) with that of ribose, exhibiting an order of magnitude lower value $6\text{x}10^{-20}$ cm^2, (Shchukin et al., 2013) leads to conclusion that H-atom loss from the thymine moiety would be preferable. Previously, the cross sections for the $[M–H]^-$ ions in thymine and thymidine were measured repeatedly. Thus, for the $[M–H]^-$ ions in at 1.7 eV in thymine, the values of $3\text{x}10^{-19}$ cm^2 (total DEA cross section) (Aflatooni et al., 2006) and $6\text{x}10^{-16}$ cm^2 (Denifl et al., 2003) were obtained. In the case of thymidine, the cross section is $1.8\text{x}10^{-18}$ cm^2 (Ptasińska et al., 2006) and $1.6\text{x}10^{-18}$ cm^2 (Abdoul-Carime et al., 2004a,b). It should be noted that our data, as well as the literature data, are somewhat different from each other. As noted in work (Aflatooni et al., 2006), the probable cause of the discrepancies is due to unavoidable errors in estimating the pressure directly in the molecular beam.

To locate the weakest hydrogen binding site more explicitely, the

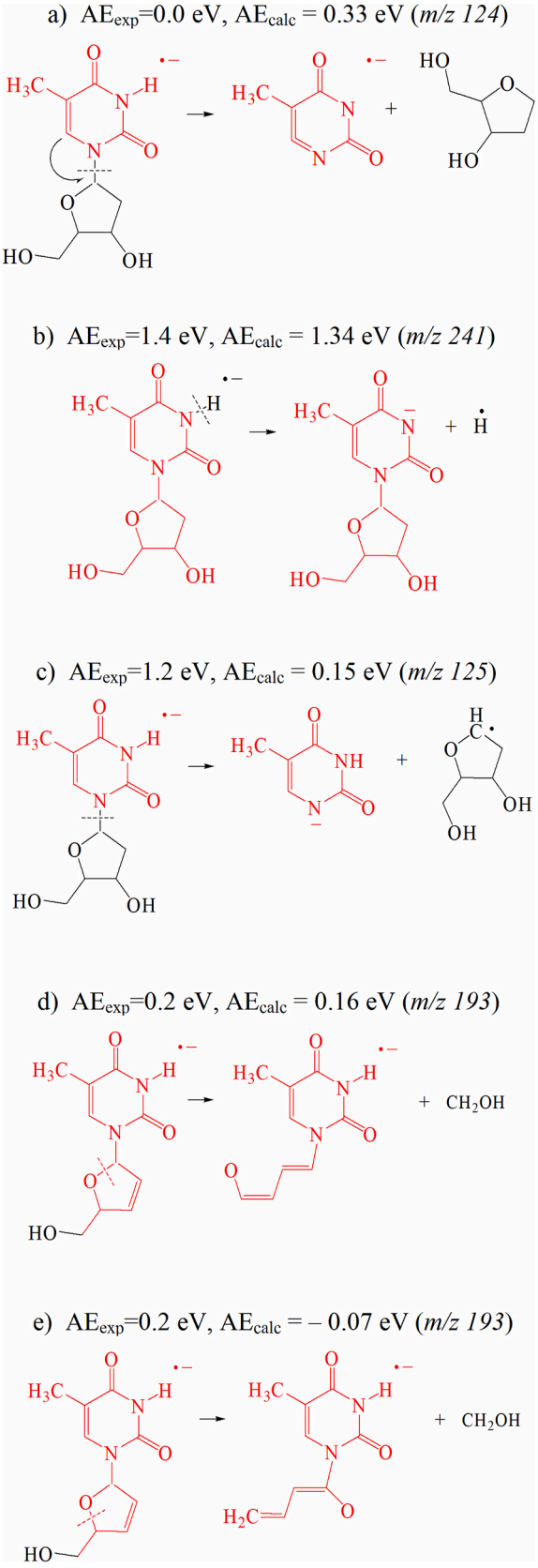

Fig. 2. Dissociative electron attachment reactions in thymidine and stavudine leading to formation of selected fragment negative ions (see text). The figure shows calculated (AE_{calc}) and experimental estimated (AE_{exp}) appearance energies and mass numbers of produced ions (m/z).

quantum-chemical calculations were performed. The $[M–H]^-$ ions appearance energy for hydrogen atom loss from N_3 position is assessed to constitute 1.34 eV, whilst greater energy is needed for H loss from C_6 sites of the pyrimidine ring (1.69 eV) and from methyl group (2.48 eV). Therefore, the lowest-threshold H-atom loss from N_3 site is accepted the most probable (Fig. 2b). This proved the similar conclusion by Ptasińska et al. (2006) made from the comparison of the $[M–H]^-$ ion yield features for thymidine and methylated thymine.

The next strongest fragmentation channel in the low energy region corresponds to the $[M–R]^-$ ions (m/z 125), exhibiting the resonant peaks at 1.8 and 3.6 eV (Fig. 1). Ptasinska et al.(Ptasińska et al., 2006) found the $[M–R]^-$ ions yield to be temperature dependent all over the energy range below 5 eV. They concluded that the appearance of $[M–R]^-$ ions in this low-energy region was caused by thermal decomposition of the sample. The issue concerning the possible ways of thermal decomposition of nucleosides has been experimentally analysed in detail in our previous work (Muftakhov and Shchukin, 2018), and an implication of residuals of water inevitably present in the samples has been established. In the present experiments, to avoid this effect, the sample of thymidine was loaded into ionization chamber and preliminarily subjected to extensive drying in vacuo, by heating to lower, pre-evaporation temperature. As a result, subsequent experiments with varied temperatures (not presented) revealed no temperature dependence for $[M–R]^-$ ion peaks at 1.8 and 3.6 eV, that testifies to the emergence of them from nondecomposed thymidine molecules. The only peak that evinced legible temperature dependence was zero-energy peak. The energy threshold for N-glycosidic bond cleavage was estimated by quantum chemical calculations to amount 0.15 eV (Fig. 2c). Therefore, appearance of $[M–R]^-$ ions at zero energy should be considered spurious and can be ascribed to some extraneous process, *e.g.* to electron capture by some products of thermodestruction of thymidine. Although, another explanation could be put forward, such as the appearance of these ions below the energy threshold due to electron attachment to vibrationally excited molecules, reminiscence of the hot-band phenomena ubiquitous in optical spectroscopy.

A remarkable feature can be revealed from the comparison of reactions that produces the $[M–R]^-$ and $[M–H]^-$ anions. In the low-energy region, the yield of $[M–R]^-$ ions appear to be an order of magnitude weaker (see Fig. 1) despite the threshold energy for this dissociative channel being much more beneficial, 0.15 eV (see Fig. 2c) against 1.34 eV for H-atom loss (see above). To explain this disconformity, the mechanisms of formation of these anions ought to be examined in depth.

In the low-energy range <5 eV, anion states in thymidine are associated with the electron capture to unfilled π* molecular orbitals (single particle shape resonances). The spatial profiles of low-lying molecular π*-orbitals are sketched in Fig. 3. As can be seen, in thymidine, the π_1* and π_2* orbitals are mainly localized on the thymine moiety and no contribution from sugar fragment is observed. As for π_3* orbital, appearance of orbital density localized on the sugar fragment can be discerned, oriented so as to bring some σ*-contribution via weak π*/σ* mixing. Anyway, from this orbital analysis one can expect π* anion states of nucleoside to be almost identical to those of constituting nucleobase. Standing on this guess, the lowest by energy resonances observed in thymidine by total (integral) ion yield curve at 0.2, 1.6 and 3.6 eV (see Fig. 1) can be matched with the first three π* shape resonances found for thymine by means of electron transmission spectroscopy at 0.29 ($^2[\pi_1^*]$), 1.71($^2[\pi_2^*]$) and 4.05 eV $^2[\pi_3^*]$) (Aflatooni et al., 1998). Unfortunately, no ETS data was found for thymidine in the literature. The calculated VAEs 0.11 ($^2[\pi_1^*]$), 1.17($^2[\pi_2^*]$) and 3.35 eV $^2[\pi_3^*]$) (see Fig. 3) are in good agreement with mentioned experimental data. Thus, the $[M–H]^-$ and $[M–R]^-$ fragment ions observed in the 1.1–1.6 eV energy range should be attributed to the products of decay of the $^2[\pi_2^*]$ resonant state.

However, one more confusion arises. To be formed, both these ions, $[M–H]^-$ and $[M–R]^-$, require cleavage of C–H and C–N bonds that lie in the symmetry plane of the nucleobase moiety, but $^2[\pi_2^*]$ anion state is

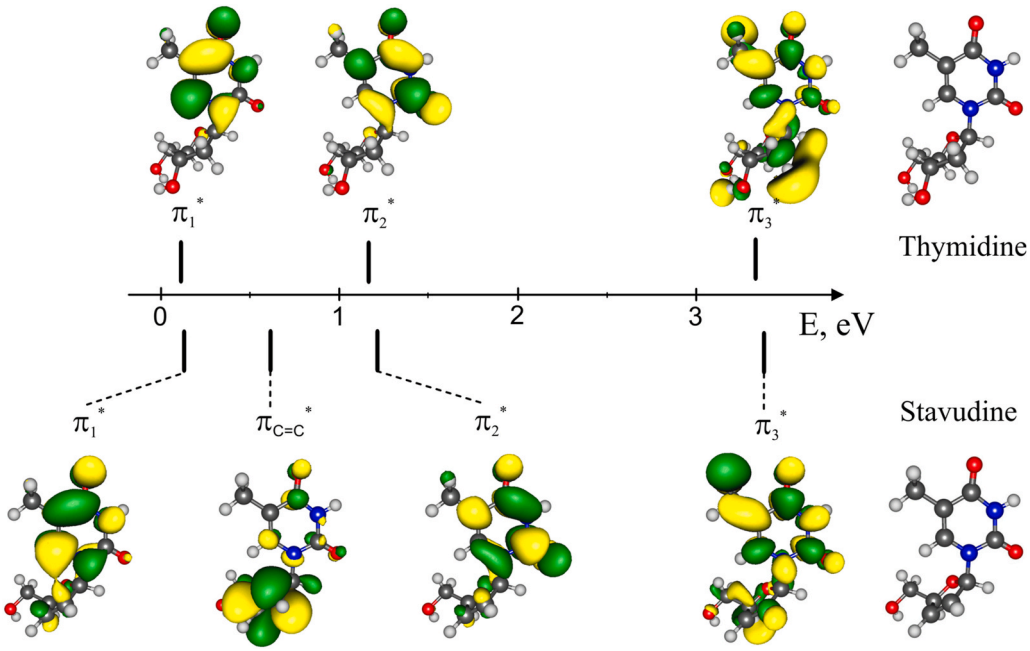

Fig. 3. Schematic view of the B3LYP/6-31G(d) unfilled π* molecular orbitals of neutral thymidine and stavudine (see text) and predicted VAEs of the corresponding negative ion states (vertical bars).

antisymmetric with respect to this plane. According to work (Khvostenko and Rafikov, 1975) symmetry of the parent electronic states must correlate with that of daughter fragments, thus the fast formation of $[M–H]^-$ and $[M–R]^-$ ions directly from $^2[\pi_2^*]$ resonant state is forbidden by the symmetry selection rule. The only worthy way to resolve this contradiction is to evoke to the predissociation mechanism (Clarke and Coulson, 1969; Scalicky et al., 2002; Vasil'ev et al., 2001), which implies vibronic coupling to promote the radiationless transitions between the electronic states. Thus the nascence of $[M–H]^-$ and $[M–R]^-$ ions may occur non-prohibitedly if to suggest transition from the initial electronic $^2[\pi_2^*]$ anion state to the finalizing dissociative $^2[\sigma^*_{C–H}]$ or $^2[\sigma^*_{C–N}]$ states, repulsive along the C–H and C–N bonds, respectively. If so, the presence of a barrier is to be assumed lying across the path to the dissociative term. The predissociative elimination of light hydrogen atom may occur both over the barrier and via permeation/tunneling through barrier (Vasil'ev et al., 2001; Shchukin et al., 2015), whereas removal of the much heavier saccharide fragment to give $[M–R]^-$ ions is less feasible since it is attainable only by the over-barrier transition (see Fig. 4), the tunneling probability being near zero. The efficiency of over-barrier transitions strongly depends both on the barrier height/-width and population of vibrational levels in the vicinity of the barrier top, that in turn depends on the relative displacement of the molecular, electron-attaching and dissociating electronic terms within the Franck-Condon region. The molecule/anion structure of thymidine is known to be rather labile, equilibrating between various molecular conformations (Yurenko et al., 2007). One can take a guess, that among the many conformers, there will certainly be several those that preform a favorable arrangement of potential curves to enable over-barrier generation of (low-yield) $[M–R]^-$ ions, while for hydrogen tunneling the need for specific conformation is less essential, thus resulting in much more abundant yield of $[M–H]^-$ ions. It is also worth to outline, that above interpretation of the differences in the yield efficiency of the $[M–R]^-$ and $[M–H]^-$ ions is prudent to be disseminated to deoxyuridine as well, for which, in the similar low-energy resonances, the yield of former ions was found six-fold less abundant, than for the latters (Muftakhov and Shchukin, 2019).

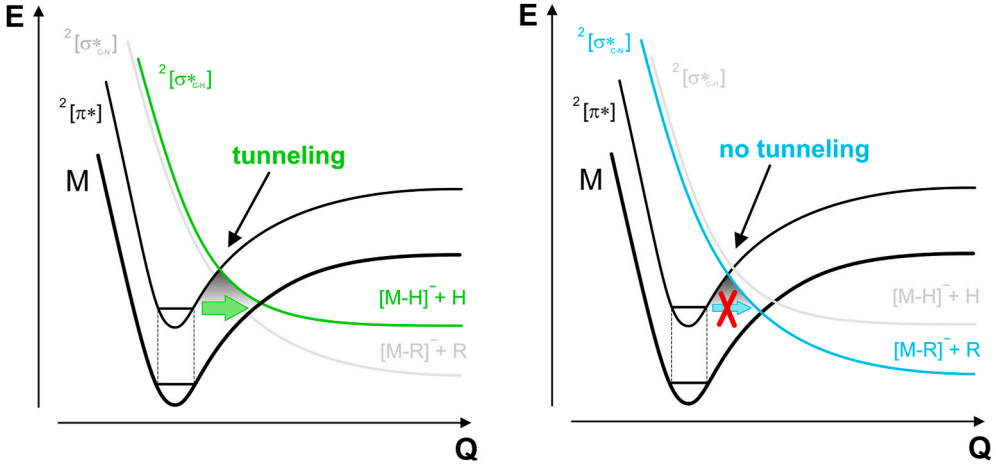

Fig. 4. Potential energy curves of a neutral molecule of thymidine (M) and anionic $^2[\pi^*]$ and $^2[\sigma^*]$ states, illustrating the formation of $[M–H]^-$ via predissociation and impossibility of such an outcome for $[M–R]^-$ ions formation (R denotes a deoxyribose fragment) (see text).

4.2. Stavudine

Resonant electron capture mass spectrum of stavudine comprises as many as twenty fragment negative ions peaks, the effective yield curves of which are shown in Fig. 5. As in thymidine, no molecular ions peak was observed. Regardless the detectability of much more fragmentation channels, within the high-energy range >5 eV the total dissociative electron attachment cross section is only 1.5 times greater than that for thymidine, the dominant contribution being from the OCN^- ions (m/z = 42). Some of the observed ions from stavudine clearly originate by similar routs as for thymidine (cf. $[M–H]^-$, $[M–R]^-$, $[M–RH]^-$, $[M–R–CO]^-$, OCN^- ions in Figs. 1 and 5). Other majority of fragment ions appear in the energy range above 4 eV, therefore unambiguous identification of their structures and/or neutral counterparts by thermochemical calculations is difficult. Just like in thymidine, the dominant fragmentation channels of stavudine molecular anions result in the formation of the $[M–H]^-$ (m/z = 223), $[M–R]^-$ (m/z = 125, where R = $C_5H_7O_2$ is a modified sugar moiety) and OCN^- species. However, in contrast to thymidine, the yield of $[M–R]^-$ ions in stavudine in the low-energy range is extremely intense. Among the other ions formed in both compounds, notable difference is due to appearance of $[M–RH]^-$ (m/z 124) and $[M–R–CO]^-$ (m/z 97) ions. The group of ions with m/z 84–81 has also no analogues in the mass spectra of thymidine and thymine, so all of them should inevitably be attributed to the species arising due to the modification of the sugar moiety. Judging from the heavy elemental composition of the ions with m/z 150, they apparently comprise partially destructed both parts of stavudine, modified sugar and thymine, with N-glycosidic bond remaining unbroken. Negative ions with m/z 54 were previously observed for thymine (Denifl et al., 2004b), therefore, by analogy they may be associated with a fragmented nucleobase, having the atomic composition of $C_3NH_4^-$ or $C_3OH_2^-$.

As mentioned above, the processes of ion formation in the low-energy range are of particular interest, since their study can shed some light on the mechanism of biochemical reactions in living cells. In the low-energy range, in addition to $[M–H]^-$ ions with m/z 223, which is subject to attribute to the loss of H-atom from N_3 site as in thymidine, there are two abundant peaks with m/z 193 and m/z 125 ($[M–R]^-$) (Fig. 5). The former is easy to attribute to $[M–CH_2OH]^-$ ions resulted by the detachment of a hydroxymethyl group from a sugar moiety, but surprisingly no similar peak with expected m/z = 211 was observed in thymidine (see Fig. 1). If to suppose simple bond cleavage, the appearance of $[M–CH_2OH]^-$ ions from stavudine requires rather high electron energy, the calculated threshold AE_{calc} being at least 1.77 eV. Moreover, the resultant $[M–CH_2OH]^-$ ion is predicted by quantum chemical calculations to be unstable with respect to further decay via dissociation of the weakest N-glycosidic bond. Thus, observation of discussed ions at energies below the aforementioned theoretical threshold indicates that they are more likely produced via preliminary isomerization of the anion structure. Indeed, the presence of fragment ion peaks with m/z 84–81 in the mass spectrum of stavudine unequivocally testify to the fragmentation of molecular ions caused by the opening of the sugar ring. If so, it cannot be ruled out that the $[M–CH_2OH]^-$ ions arise due to the occurrence of a linear form of sugar. The opening of the sugar ring can occur as a result of ruptures of $C_{1'}$ –O or $C_{4'}$ –O bonds. The expected most stable structures for $[M–CH_2OH]^-$ ions are shown in Fig. 2d and 2e, respectively. As can be seen, the threshold energies assessed for the corresponding dissociative reactions are relatively low, what is provided by stabilizing effect of nascent conjugation of double-bonds. However, such a route proceeds through rearrangements and fragmentation takes longer time, therewith undergoing strong competition from electron autodetachment. That is why the yield of $[M–CH_2OH]^-$ ions may turn out to be weaker compared to $[M–R]^-$ ions formed faster, by simple bond cleavage.

As mentioned above, the most striking dissimilarity of the resonant electron capture by stavudine from that of thymidine lies in the enormously abundant yield of $[M–R]^-$ ions in the low-energy range. Albeit they obviously originate from the similar $^2[\pi^*]$ resonances, absolute formation cross section for these ions is more than two orders (!) of magnitude as much as that for the same ions from thymidine. Also, the $[M–R]^-$ ions effective yield curve exhibits an additional resonance peak at 0.78 eV with a cross section of ~ $3.6x10^{-17}$ cm^2. We believe that this specific feature is caused by the presence of a C=C double bond in the sugar ring, which alters the electronic structure of the molecule as described below.

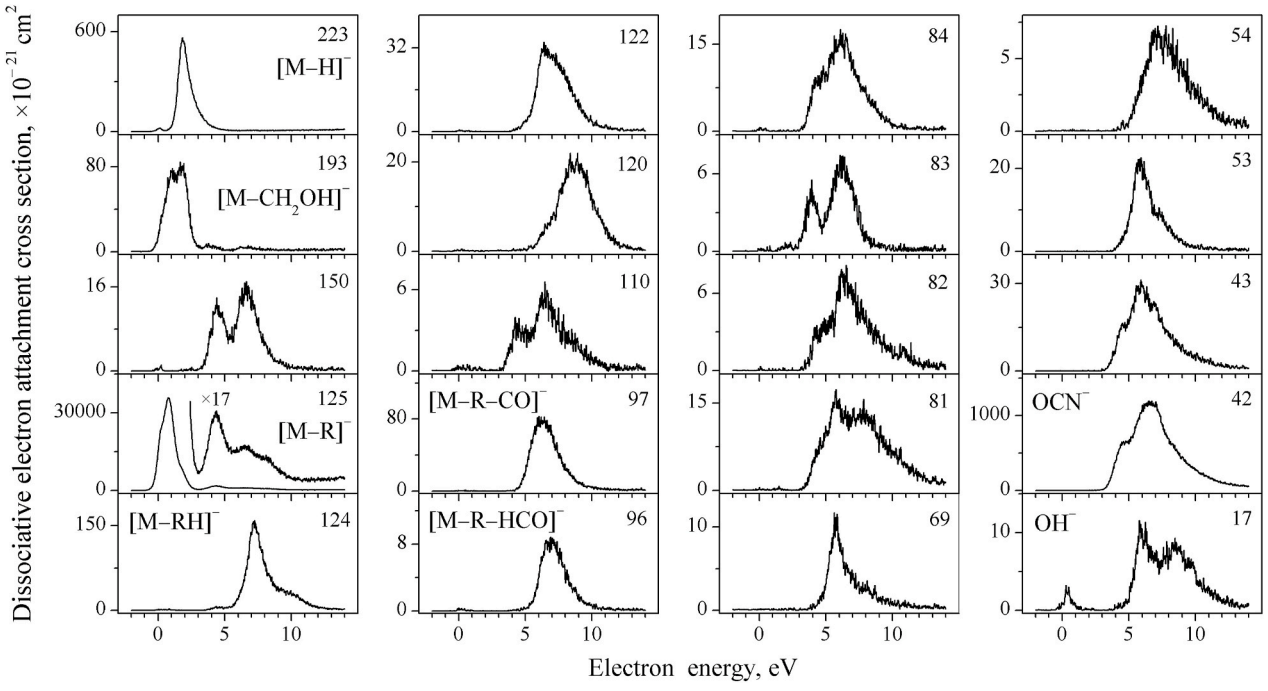

Fig. 5. Formation cross sections for negative ions from stavudine as functions of electron energy. Mass numbers of ions (m/z) are indicated on the upper right corner of each panel. The R stands for $C_5H_7O_2$ neutral counterpart representing modified deoxyribose radical.

The general view of the empty π* orbitals of neutral stavudine molecules as predicted by B3LYP/6-31G* calculations are shown in Fig. 3 π_1*, π_2*, and π_3* symbolize the series of empty molecular orbitals antisymmetric with respect to the plane of the nucleobase moiety. Having similar nodal properties, these molecular orbitals look almost identical to those of thymidine. Thus, close similarity can be expected for stavudine and thymidine both in the disposition of these $^2[\pi^*]$ shape resonances and their dissociative consequences. Indeed, calculated VAEs at 0.14, 1.22, and 3.39 eV confirm this expectation by showing a good agreement with resonance peaks observed in the total ion yield efficiency curves of stavudine at 0.1 eV, 1.8 eV, and 4.0 eV (see Fig. 3). It seems prudent to ascribe the appearance of an additional resonance in stavudine at an energy ca. 0.8 eV to the interposition of one more molecular orbital. Indeed, the only differing structural feature, the presence of C=C double bond in the sugar moiety instead of single bond in thymidine, gives an additional π* orbital localized mainly around the C=C bond region (marked as $\pi^*_{C=C}$ in Fig. 3). Thus, the resonance peak on the $[M–R]^-$ ion yield curve at an energy 0.78 eV is to be attributed to the $^2[\pi^*_{C=C}]$ single-particle shape resonance, matching to the calculated VAE of 0.61 eV (see Fig. 3).

As can be seen from orbital profile, the $\pi^*_{C=C}$ molecular orbital partially mixes with σ* orbitals, antisymmetric with respect to the plane of the sugar moiety, including those localized on the C–N glycosidic bond (see Fig. 3). As a result of this mixing, at capture of an electron to the (Cobut et al., 1998)$[\pi^*_{C=C}]$ anionic state a direct rupture of the C–N bond becomes possible, avoiding the need for intermediary predissociative transition as shown above for thymidine. Apparently, that is why in stavudine the fragmentation to give ions $[M–R]^-$ at an energy of 0.78 eV proceeds with such a high efficiency. Furthermore, in contrast to thymidine, the π_1*, π_2* and π_3* orbitals of the nucleobase moiety in stavudine on closer inspection exhibit also some visible contributions in the C=C area of the sugar moiety, bridging with it via involving N-glycosidic bond (see Fig. 3). As a consequence, production of $[M–R]^-$ ions from the all three resonances in $^2[\pi_1^*]$, $^2[\pi_2^*]$ and $^2[\pi_3^*]$ anionic states happens to be much more efficient than in thymidine. At the same time, the higher lying (presumably, core-excited) resonances observed for both compounds at ca. 6.3 and 8 eV give the $[M–R]^-$ yields of essentially equal absolute cross sections (cf. Figs. 1 and 5). Continuing to analyze the lowest-energy π* orbitals under question, it is notable that the presence of double bond in sugar moiety of stavudine does not have any effect on orbital densities along C–H bonds in nucleobase moiety, leaving them still zero. Therefore the need for predissociation to form $[M–H]^-$ ions remains equally actual, as for thymidine. Indeed, the measured absolute cross sections for the formation of $[M–H]^-$ ions from both nucleosides justify such a scenario by exhibiting approximately the same values (cf. Figs. 1 and 5).

5. Summary and conclusion

For thymidine and stavudine, the processes of low-energy (0-14 eV) electron-molecule interaction resulting in resonant electron attachment with subsequent negative ion formation were studied. The composition of negative ion mass spectra of thymidine have much in common with that of the previously studied deoxyuridine, the lack of long-lived molecular ion peaks being inclusive. In particular, comparing mass spectra of thymidine and deoxyuridine (Muftakhov and Shchukin, 2019) one can conclude that methyl substitution in the nucleobase has almost no effect on fragmentation of molecular negative ions. Another important finding is the absence of $[M–CH_3]^-$ ions in the thymidine mass spectrum, that could imitate the conversion of thymine to uracil. This means that the low-energy electron induced processes can hardly be responsible for mutations in the DNA sequence via conversion thymine to uracil.

In the lower electron energy region the negative ions both from thymidine and stavudine are formed due to the single-particle π* shape resonances. The latter are associated with the electron capture to π* molecular orbitals localized mainly on the nucleobase part, but for stavudine one more resonance appear due to the sugar moiety being modified and having C=C double bond. On the whole, the mainstream dissociative electron attachment channels for both compounds are H-atom elimination and the N-glycosidic bond cleavage yielding (dehydrogenated) thymine anions. In the low-energy region, however, the N-glycosidic bond cleavage reaction in thymidine is much less effective, in spite of the gainful threshold energy than that for H-atom elimination. Such a discrimination is explained by the specific symmetry ban imposed to dissociative decay of the antysimmetric π*-anionic states by means of breaking of a σ-bond, symmetric with respect to the plain of decaying anionic moiety. Lifting of the ban may occur via predissociation toward adjacent σ*-state. It proceeds much more efficiently when light H-atom is eliminating because of its easy tunneling capability through the barrier, whereas the heavy neutral sugar fragment can be expelled exclusively over the barrier.

The resonant electron capture by stavudine differs significantly from that for deoxyuridine and thymidine. In the high-energy region >5 eV some new fragmentation channels appear. In sharp contrast to thymidine, when compared in absolute cross section units, the yield of thymine anions ($[M–R]^-$) from stavudine in the lower electron energy region <5 eV is found to be unexpectedly almost three orders of magnitude higher (Figs. 1 and 5). Obviously, this is due to the presence of C=C double bond in a modified sugar fragment which alters the molecular electronic structure. Intrusion of the additional $\pi^*_{C=C}$ molecular orbital mixed with other orbitals provides an intense N-glycosidic bond cleavage resulting in the rather high abundance of $[M–R]^-$ ions.

Stavudine is an antiretroviral drug for treating and preventing HIV infection. One of the notorious complications of HIV and AIDS is the emergence of cancer. In the light of presently revealed instability of stavudine towards incident low-energy electron, the question arises of its compatibility with radiation therapy, which often used for cancer treatment. Indeed, it is well known fact that primary radiation generates in the organism a wealth of secondary low-energy electrons, which can be captured by the stavudine molecules as well. Can't the dissociative attachment of secondary electrons result in the damage of stavudine molecules and thereby block its therapeutic effect as an antiretroviral drug? In the same vein, another question arises of a diametrically opposite purport. The ability of nucleoside analogues (with the modified sugar incorporated) to efficiently decay when faced with the low-energy electron, on the contrary, might be used for medicinal purposes. Indeed, modified nucleotides are already used as radiosensitizers, compounds that increase the sensitivity of tumor cells against exposed radiation. The mechanism of their action lies in their incorporation into tumor DNA instead of native nucleotides. Unlike the latter, modified nucleotide may effectively decompose due to the attachment of secondary electrons generated by the ionizing radiation, therewith ultimately killing the tumor cell. Among the radiosensitizers, one of the best known nucleoside analogue is bromouridine. The dissociative electron attachment study of this compound revealed the effective fragmentation in the low-energy region, yielding the Br^- and $[BrU–H]^-$ ions with the cross sections of $2x10^{-14}$ cm^2 and $9x10^{-16}$ cm^2, respectively (Abdoul-Carime et al., 2004b). At present, the searching of new potential radiosensitizers suitable for cancer therapy is challenging task, but the range of such compounds is still expanding (Sosnowska et al., 2017; Spisz et al., 2019; Schürmann et al., 2017; Ameixa et al., 2018; Meißner et al., 2019). To raise the susceptibility to secondary low-energy electrons the molecules of radiosensitizers should be good electrophores, what is provided by a relatively high molecular electron affinity. On the other side, among the criteria for the effectiveness of radiosensitizers is their capacity for intense electron-induced fragmentation to produce reactive radicals that result in cancer DNA strand breaks (Chomicz et al., 2013). Therefore, in order to improve antitumor activity, nucleosides are modified by the introduction of substituents on the nucleobase at the atoms free of hydrogen bonds retaining the DNA helix (for example, at C_5 site of the pyrimidine ring of uracil nucleobase (Meißner et al., 2019)). However,

this approach has its limitations, since the introduction of large functional group can significantly alter the molecular structure and therewith the functionality of the nucleoside. In this sense, the revealed instability of stavudine in the dissociative low-energy electron attachment reactions may be significative clue, since it is achieved without changing the nucleobase fragment, but only by modifying the sugar moiety. Of no less importance is that modification of thymidine, a predecessor of stavudine, is achieved with minimal structural changes in the molecular geometry.

Summarizing, thus discovered by the example of stavudine the enhancement of low-energy electron-induced fragmentation due to modification of sugar moiety is worth receiving attention when designing new radiosensitizers, promising alternatives to halogenated radiosensitizers.

Author contribution statement

Mars V. Muftakhov: supervised the project, wrote the paper with input from all authors. Pavel V. Shchukin: conceived the original idea, carried out the experiment, interpretation of the results. Rustem V. Khatymov: performed the quantum chemical calculations.

Declaration of competing interest

The authors declare that they have no known competing financial interests or personal relationships that could have appeared to influence the work reported in this paper.

Appendix A. Supplementary data

Supplementary data to this article can be found online at https://doi.org/10.1016/j.radphyschem.2021.109464.

References

Abdoul-Carime, H., Gohlke, S., Fischbach, E., Scheike, J., Illenberger, E., 2004a. Thymine excision from DNA by subexcitation electrons. Chem. Phys. Lett. 387, 267. https://doi.org/10.1016/j.cplett.2004.02.022.

Abdoul-Carime, H., Limão-Vieira, P., Gohlke, S., Petrushko, I., Mason, N.J., Illenberger, E., 2004b. Sensitization of 5-bromouridine by slow electrons. Chem. Phys. Lett. 393, 442. https://doi.org/10.1016/j.cplett.2004.06.081.

Aflatooni, K., Gallup, G.A., Burrow, P.D., 1998. Electron attachment energies of the DNA bases. J. Phys. Chem. 102, 6205. https://doi.org/10.1021/jp980865n.

Aflatooni, K., Scheer, A.M., Burrow, P.D., 2006. Total dissociative electron attachment cross sections for molecular constituents of DNA. J. Chem. Phys. 125, 054301 https://doi.org/10.1063/1.2229209.

Ameixa, J., Arthur-Baidoo, E., Meißner, R., Makurat, S., Kozak, W., Butowska, K., Ferreira da Silva, F., Rak, J., Denifl, S., 2018. Low-energy electron-induced decomposition of 5-trifluoromethanesulfonyl-uracil: a potential radiosensitizer. J. Chem. Phys. 149, 164307. https://doi.org/10.1063/1.5050594.

Babadaei, M.M.N., Hasan, A., Vahdani, Y., Bloukh, S.H., Sharifi, M., Kachooei, E., Haghighat, S., Falahati, M., 2020. Development of remdesivir repositioning as a nucleotide analog against COVID-19 RNA dependent RNA polymerase. J. Biomol. Struct. Dyn. 1–9. https://doi.org/10.1080/07391102.2020.1767210.

Bald, I., Kopyra, J., Illenberger, E., 2006. Selective excision of C5 from D-ribose in the gas phase by low-energy electrons (0–1 eV): implications for the mechanism of DNA damage. Angew. Chem. Int. Ed. 45, 4851. https://doi.org/10.1002/anie.200600303.

Boudaïffa, B., Cloutier, P., Hunting, D., Huels, M.A., Sanche, L., 2000. Resonant formation of DNA strand breaks by low-energy (3 to 20 eV) electrons. Science 287, 1658. https://doi.org/10.1126/science.287.5458.1658.

Chomicz, L., Zdrowowicz, M., Kasprzykowski, F., Rak, J., Buonaugurio, A., Wang, Y., Bowen Jr., K.H., 2013. How to find out whether a 5-substituted uracil could be a potential DNA radiosensitizer. J. Phys. Chem. Lett. 4 (17) https://doi.org/10.1021/jz401358w, 2853.

Clarke, D.D., Coulson, C.A., 1969. The dissociative breakdown of negative ions. J. Chem. Soc. A 1, 169. https://doi.org/10.1039/J19690000169.

Cobut, V., Frongillo, Y., Patau, J.P., Goulet, T., Fraser, M.-J., Jay-Gerin, J.-P., 1998. Monte Carlo simulation of fast electron and proton tracks in liquid water. I. Physical and physicochemical aspects. Radiat. Phys. Chem. 51, 229. https://doi.org/10.1016/S0969-806X(97)00096-0.

Denifl, S., Ptasińska, S., Hanel, G., Gstir, B., Probst, M., Scheier, P., Märk, T.D., 2004a. Electron attachment to gas-phase uracil. J. Chem. Phys. 120, 6557. https://doi.org/10.1063/1.1649724.

Denifl, S., Ptasińska, S., Probst, M., Hrušák, J., Scheier, P., Märk, T.D., 2004b. Electron attachment to the gas-phase DNA bases cytosine and thymine. J. Phys. Chem. 108, 6562. https://doi.org/10.1021/jp049394x.

Denifl, S., Ptasinska, S., Cingel, M., Matejcik, S., Scheier, P., Märk, T.D., 2003. Electron attachment to the DNA bases thymine and cytosine. Chem. Phys. Lett. 377, 74–80. https://doi.org/10.1016/S0009-2614(03)01096-0.

Gohlke, S., Rosa, A., Illenberger, E., Brüning, F., Huels, M.A., 2002. Formation of anion fragments from gas-phase glycine by low energy 0–15 eV electron impact. J. Chem. Phys. 116, 10164. https://doi.org/10.1063/1.1479348.

Gohlke, S., Abdoul-Carime, H., Illenberger, E., 2003. Dehydrogenation of adenine induced by slow (<3 eV) electrons. Chem. Phys. Lett. 380, 595. https://doi.org/10.1016/j.cplett.2003.09.013.

Gorfinkiel, J.D., Ptasinska, S., 2017. Electron scattering from molecules and molecular aggregates of biological relevance. J. Phys. B 50, 182001. https://doi.org/10.1088/1361-6455/aa8572.

A.A. Granovsky, Firefly version 8, www.http://classic.chem.msu.su/gran/firefly/index.html.

Hanel, G., Gstir, B., Denifl, S., Scheier, P., Probst, M., Farizon, B., Farizon, M., Illenberger, E., Märk, T.D., 2003. Electron attachment to uracil: effective destruction at subexcitation energies. Phys. Rev. Lett. 90, 188104. https://doi.org/10.1103/PhysRevLett.90.188104.

http://www.xdft.org/dft/Xmethods/X1.html.

Huber, D., Beikircher, M., Denifl, S., Zappa, F., Matejcik, S., Bacher, A., Grill, V., Märk, T. D., Scheier, P., 2006. High resolution dissociative electron attachment to gas phase adenine. J. Chem. Phys. 125, 084304 https://doi.org/10.1063/1.2336775.

Hurst, M., Noble, S., 1999. Stavudine: an update of its use in the treatment of HIV infection. Drugs 58, 919. https://doi.org/10.2165/00003495-199958050-00012.

Jian-Xing, X., 2015. The electron leak pathways of mitochondrial respiratory chain and its potential application in medical research. JSM Cell Dev. Biol. 3, 1014.

Khatymov, R.V., Muftakhov, M.V., Mazunov, V.A., 2003. Phenol, chlorobenzene and chlorophenol isomers: resonant states and dissociative electron attachment. Rapid Commun. Mass Spectrom. 17, 2327. https://doi.org/10.1002/rcm.1197.

Khvostenko, V.I., 1981. Mass spektrometriya otritsatel'nykh ionov v organicheskoi khimii [Mass Spectrometry of Negative Ions in Organic Chemistry]. Nauka, Moscow, p. 159 (in Russian).

Khvostenko, V.I., Rafikov, S.R., 1975. The main rules for the formation of negative ions via dissociative electron attachment to polyatomic molecules. Dokl. Akad. Nauk SSSR 220, 892 (in Russian).

König, C., Kopyra, J., Bald, I., Illenberger, E., 2006. Dissociative electron attachment to phosphoric acid esters: the direct mechanism for single strand breaks in DNA. Phys. Rev. Lett. 97, 018105 https://doi.org/10.1103/PhysRevLett.97.018105.

Kopyra, J., König-Lehmann, C., Illenberger, E., 2013. Electron attachment to the dipeptide alanyl-glycine. Chem. Phys. Lett. 578, 54. https://doi.org/10.1016/j.cplett.2013.06.014.

Kukhanova, M.K., 2012. Anti-HIV nucleoside drugs: a retrospective view into the future. Mol. Biol. 46, 768. https://doi.org/10.1134/S002689331206012X.

Lee, M.W., Parker, W.B., Xu, B., 2013. New insights into the synergism of nucleoside analogs with radiotherapy. Radiat. Oncol. 8, 223. https://doi.org/10.1186/1748-717X-8-223.

Mazunov, V.A., Shchukin, P.V., Khatymov, R.V., Muftakhov, M.V., 2006. Negative ion mass spectrometry in resonant electron capture mode. Mass Spektrom 3, 32 (in Russian).

Meißner, R., Makurat, S., Kozak, W., Limão-Vieira, P., Rak, J., Denifl, S., 2019. Electron-induced dissociation of the potential radiosensitizer 5-selenocyanato-2'-deoxyuridine. J. Phys. Chem. B 123, 1274. https://doi.org/10.1021/acs.jpcb.8b11523.

Muftakhov, M.V., Shchukin, P.V., 2011. Dissociative electron attachment to glycyl-glycine, glycyl-alanine and alanyl-alanine. Phys. Chem. Chem. Phys. 13, 4600. https://doi.org/10.1039/C0CP00940G.

Muftakhov, M.V., Shchukin, P.V., 2013. Resonant electron capture by uridine//. J. Anal. Chem. 68, 1200. https://doi.org/10.1134/S1061934813140086.

Muftakhov, M.V., Shchukin, P.V., 2018. Destruction of peptides and nucleosides in reactions with low-energy electrons. Tech. Phys. 63, 747. https://doi.org/10.21883/JTF.2018.05.45907.2425.

Muftakhov, M.V., Shchukin, P.V., 2019. Resonant electron capture by uridine and deoxyuridine molecules: fragmentation with charge transfer. Rapid Commun. Mass Spectrom. 33, 482. https://doi.org/10.1002/rcm.8354.

Muftakhov, M.V., Vasil'ev, YuV., Mazunov, V.A., 1999. Determination of electron affinity of carbonyl radicals by means of negative ion mass spectrometry. Rapid Commun. Mass Spectrom. 13, 1104. https://doi.org/10.1002/(SICI)1097-0231(19990630)13:12<1104::AID-RCM619>3.0.CO;2-C.

Pruijssers, A.J., Denison, M.R., 2019. Nucleoside analogues for the treatment of coronavirus infections. Curr. Opin. Virol. 35, 57. https://doi.org/10.1016/j.coviro.2019.04.002.

Ptasińska, S., Denifl, S., Scheier, P., Märk, T.D., 2004. Inelastic electron interaction (attachment/ionization) with deoxyribose. J. Chem. Phys. 120, 8505. https://doi.org/10.1063/1.1690231.

Ptasińska, S., Denifl, S., Mróz, B., Probst, M., Grill, V., Illenberger, E., Scheier, P., Märk, T.D., 2005a. Bond selective dissociative electron attachment to thymine. J. Chem. Phys. 123, 124302. https://doi.org/10.1063/1.2035592.

Ptasińska, S., Denifl, S., Candori, P., Matejcik, S., Scheier, P., Märk, T.D., 2005b. Dissociative electron attachment to gas phase alanine. Chem. Phys. Lett. 403, 107. https://doi.org/10.1016/j.cplett.2004.12.115.

Ptasińska, S., Denifl, S., Gohlke, S., Scheier, P., Illenberger, E., Märk, T.D., 2006. Decomposition of thymidine by low-energy electrons: implications for the molecular

mechanisms of single-strand breaks in DNA. Angew. Chem. Int. Ed. 45, 1893. https://doi.org/10.1002/anie.200503930.

Scalicky, T., Chollet, C., Pasquier, N., Allan, M., 2002. Properties of the π* and σ* states of the chlorobenzene anion determined by electron impact spectroscopy. Phys. Chem. Chem. Phys. 4, 3583. https://doi.org/10.1039/B202494B.

Scheer, A.M., Burrow, P.D., 2006. π* orbital system of alternating phenyl and ethynyl groups: measurements and calculations. J. Phys. Chem. B 110, 17751–17756. https://doi.org/10.1021/jp0628784.

Schmidt, M.W., Baldridge, K.K., Boatz, J.A., Elbert, S.T., Gordon, M.S., Jensen, J.H., Koseki, S., Matsunaga, N., Nguyen, K.A., Su, S., Windus, T.L., Dupuis, M., Montgomery, J.A., 1993. General atomic and molecular electronic structure system. J. Comput. Chem. 14, 1347. https://doi.org/10.1002/jcc.540141112.

Schürmann, R., Tanzer, K., Dąbkowska, I., Denifl, S., Bald, I., 2017. Stability of the parent anion of the potential radiosensitizer 8-bromoadenine formed by low-energy (<3 eV) electron attachment. J. Phys. Chem. B 121, 5730. https://doi.org/10.1021/acs.jpcb.7b02130.

Seley-Radtke, K.L., Yates, M.K., 2018. The evolution of nucleoside analogue antivirals: a review for chemists and non-chemists. Part 1: early structural modifications to the nucleoside scaffold. Antivir. Res. 154, 66. https://doi.org/10.1016/j.antiviral.2018.04.004.

Shchukin, P.V., Muftakhov, M.V., Khatymov, R.V., 2013. Dissociative capture of thermal electrons by ribose and deoxyribose. Mass Spectrom. 10, 158 (in Russian).

Shchukin, P.V., Mikhailov, G.P., Muftakhov, M.V., 2015. Isotope effect in cross-section of $(M–H/D)^-$ negative ions formation from CF_3COOH and CF_3COOD. Int. J. Mass Spectrom. 380, 1. https://doi.org/10.1016/j.ijms.2015.02.002.

Sosnowska, M., Makurat, S., Zdrowowicz, M., Rak, J., 2017. 5-Selenocyanatouracil: a potential hypoxic radiosensitizer. electron attachment induced formation of selenium centered radical. J. Phys. Chem. B 121, 6139. https://doi.org/10.1021/acs.jpcb.7b03633.

Spisz, P., Zdrowowicz, M., Makurat, S., Kozak, W., Skotnicki, K., Bobrowski, K., Rak, J., 2019. Why does the type of halogen atom matter for the radiosensitizing properties of 5-halogen substituted 4-thio-20 -deoxyuridines? Molecules 24, 2819. https://doi.org/10.3390/molecules24152819.

Stokes, S.T., Li, X., Grubisic, A., Ko, Y.J., Bowen, K.H., 2007. Intrinsic electrophilic properties of nucleosides: photoelectron spectroscopy of their parent anions. J. Chem. Phys. 127, 084321 https://doi.org/10.1063/1.2774985.

Sulzer, P., Ptasinska, S., Zappa, F., Mielewska, B., Milosavljevic, A.R., Scheier, P., Märk, T.D., 2006. Dissociative electron attachment to furan, tetrahydrofuran, and fructose. J. Chem. Phys. 125, 044304 https://doi.org/10.1063/1.2222370.

Vasil'ev, Y.V., Muftakhov, M.V., Tuimedov, G.M., Khatymov, R.V., Abzalimov, R.R., Mazunov, V.A., Drewello, T., 2001. Specific formation of $(M–H)^-$ ions from OH-group-containing molecules. Int. J. Mass Spectrom. 205, 119. https://doi.org/10.1016/S1387-3806(00)00289-X.

Vasil'ev, Y.V., Figard, B.J., Voinov, V.G., Barofsky, D.F., Deinzer, M.L., 2006. Resonant electron capture by some amino acids and their methyl esters. J. Am. Chem. Soc. 128, 5506. https://doi.org/10.1021/ja058464q.

Wu, J., Xu, X., 2007. The X1 method for accurate and efficient prediction of heats of formation. J. Chem. Phys. 127, 214105. https://doi.org/10.1063/1.2800018.

Yurenko, Y.P., Zhurakivsky, R.O., Ghomi, M., Samijlenko, S.P., Hovorun, D.M., 2007. How many conformers determine the thymidine low-temperature matrix infrared spectrum? DFT and MP2 quantum chemical study. J. Phys. Chem. B 111, 9655. https://doi.org/10.1021/jp073203j.